NASA TN D-1371

TECHNICAL NOTE

D-1371

PRESSURE DISTRIBUTIONS ON TWO-DIMENSIONAL SHARP-LEADING-EDGE FLAT PLATES WITH SWEEP ANGLES OF 0°, 30°, AND 45° AT A MACH NUMBER OF 6 AND ANGLES OF ATTACK FROM 0° TO 90°

By James G. Hondros

Langley Research Center
Langley Station, Hampton, Va.

NATIONAL AERONAUTICS AND SPACE ADMINISTRATION

WASHINGTON

September 1962

NATIONAL AERONAUTICS AND SPACE ADMINISTRATION

TECHNICAL NOTE D-1371

PRESSURE DISTRIBUTIONS ON TWO-DIMENSIONAL SHARP-LEADING-EDGE FLAT PLATES WITH SWEEP ANGLES OF 0°, 30°, AND 45° AT A MACH NUMBER OF 6 AND ANGLES OF ATTACK FROM 0° TO 90°

By James G. Hondros

SUMMARY

An investigation has been conducted in the Langley 20-inch Mach 6 tunnel on three two-dimensional sharp-leading-edge flat plates with sweep angles of 0°, 30°, and 45° at Reynolds numbers per foot from 7.8×10^6 to 9.6×10^6. The results indicate that there is essentially no effect of sweep angle on the pressure distributions in the attached-shock regime up to an angle of attack of about 32°. In the detached-shock regime, the major effects of sweep are generally confined to angles of attack from 43° to 70°. Free-stream stagnation pressures were measured on the 0° swept-flat-plate model at angles of attack as low as 45°, whereas stagnation pressures were not measured on the 30° and 45° swept-flat-plate models until angles of attack of about 64° and 70°, respectively. Beyond approximately 70° angle of attack the maximum pressure coefficients for all plates remain constant and sweep effects are negligible.

Predictions of the model pressures obtained from oblique-shock theory are in good agreement with the measured data in the attached-shock regime. A prediction of the maximum plate pressures obtained in the detached-shock regime and developed in the present paper by utilizing the Mach number component normal to the plate leading edge is in fair agreement with the measured data. A maximum difference of 0.1 in pressure coefficient is obtained except in the immediate region of shock detachment.

A modified Newtonian theory (maximum pressure coefficient behind a normal shock of 1.818) is ineffective in predicting the maximum measured pressures except at 90° angle of attack; whereas, the flat-plate modified Newtonian theory (maximum pressure coefficient equal to ratio of specific heats plus 1) gives a fairly good prediction in the low angle-of-attack range up to about 40°.

INTRODUCTION

The delta-wing planform appears desirable for incorporation into hypersonic gliders because of its lift capability and lower leading-edge heating characteristics. The effects of sweepback angle on the forces, pressure distributions, and heat transfer to delta-wing configurations are currently under investigation at the Langley Research Center. Previous investigations in this field are available in references 1, 2, and 3.

As a corollary to the delta-wing program, it is desirable to determine at hypersonic speeds the extent of the effects of sweep angle on the pressure distributions on two-dimensional swept-wing sections. Therefore, a program has been initiated to determine these effects through an angle-of-attack range from 0° to 90°. There is also current interest in the fact that stagnation pressures are attained and can be measured on flat-plate bodies and bodies of revolution with sharp leading edges or noses at angles of attack considerably less than 90°, as shown, for example, in reference 3. In the present investigation, a group of three two-dimensional flat-plate models having sweep angles of 0°, 30°, and 45° were tested at a Mach number of 6 and angles of attack from 0° to 90° to determine the effect of sweep angle on these maximum measured stagnation pressures. These tests were conducted in the Langley 20-inch Mach 6 tunnel at Reynolds numbers per foot from 7.8×10^6 to 9.6×10^6. Theoretical predictions are presented where applicable.

SYMBOLS

c	chord, in.
C_p	pressure coefficient, $\dfrac{2(p_l - p_\infty)}{\gamma p_\infty M^2}$
$C_{p,max}$	maximum pressure coefficient behind normal shock, $\dfrac{2(p_t - p_\infty)}{\gamma p_\infty M^2}$
M	Mach number
p_l	local measured pressure, lb/sq in. abs
p_t	total pressure behind normal shock, lb/sq in. abs

p_∞ free-stream static pressure, lb/sq in. abs

x distance from leading edge of plate in plane of free-stream velocity vector, in.

α plate angle of attack measured in streamwise plane, deg

γ ratio of specific heats

Λ sweep angle, deg

APPARATUS AND METHODS

This investigation was conducted in the Langley 20-inch Mach 6 tunnel with Reynolds number per foot varying from 7.8×10^6 to 9.6×10^6 at tunnel stagnation pressures from 400 to 515 lb/sq in. absolute and stagnation temperatures from 400° F to 420° F. The tunnel, which is described in reference 4, is a blowdown-to-atmosphere type capable of operation at a maximum stagnation pressure of 580 lb/sq in. absolute and a maximum stagnation temperature of 600° F.

The models used in this investigation consisted of three two-dimensional 1/2-inch-thick flat plates with wedge leading edges and sweep angles of 0°, 30°, and 45°. All models had sharp leading edges (0.0002 inch thick) with wedge angle of 25°, a constant 3-inch chord in streamwise planes, and a span of 12 inches in the plane normal to the free-stream velocity vector. On all models there were eight orifices located on a midspan, streamwise, pressure station. In addition, there were four orifices located about 1 and 2 inches downstream from the leading edge and 1 inch on each side of the midspan station to check two dimensionality of the flow over the wings. Model dimensions and orifice locations are presented in figure 1.

The models were mounted in the tunnel on the 90° angle-of-attack support system shown in figure 2 which pitched the model in the vertical plane. A vertical movement of the entire support system is available so that the model at an angle of attack can be located as close to the center of the tunnel as possible. The angle of attack was optically measured by using a prism mounted in the model tip to reflect light from an approximate point source to a calibrated screen in order to reduce any error derived from air loads on the model and support system.

Model pressure data were recorded by using 0 to 1 and 0 to 15 lb/sq in. absolute pressure transducers simultaneously. Tunnel stagnation pressures were recorded by using a 0 to 600 lb/sq in. absolute

transducer. The maximum error in the measured pressures is believed to be within 1 percent of the full-scale readings of the low pressure (0 to 1 lb/sq in. absolute) transducer and within 1/2 percent of the 0 to 15 and 0 to 600 lb/sq in. absolute transducers. Angles of attack are accurate to within ±30'.

The Mach number in the Langley 20-inch Mach 6 tunnel is uniform within ±0.02 throughout the test region; however, it does exhibit a slow variation with time from a value of 6.03 to 5.94. At the low angles of attack, the measured pressures were reduced to coefficient form based upon an assumed Mach number of 6.00 which would yield a maximum uncertainty of ±2 percent in dynamic pressure. At the higher angles of attack, which occurred during the latter part of each test, the Mach number was determined from the maximum measured surface pressure which was assumed to be equal to the stagnation pressure behind a normal shock provided the resulting Mach number was within the calibrated range of the nozzle, and coefficients were obtained based on this Mach number.

RESULTS AND DISCUSSION

Typical schlieren photographs of the 0° swept-flat-plate model are presented in figure 3. Presented in figures 4, 5, and 6 are the basic pressure distributions at angles of attack on the 0°, 30°, and 45° swept plates, respectively. A prediction using the boundary-layer self-induced pressure method of reference 5 (fig. 7) seems to be in fairly good agreement with measured data at 0° angle of attack. This figure also tends to indicate that the upper-surface pressures are not affecting the plate pressures or the boundary layer since the predicted values of pressure are higher than the measured values. The pressure distributions presented in figures 4 to 6 in general show very similar trends throughout the 0° to 90° angle-of-attack range for the three sweep angles. At the lower angles of attack, before shock detachment, the distributions are almost linear and show very little pressure difference from leading edge to trailing edge. Immediately after shock detachment, the pressures peak near the leading edge as the surface flow goes subsonic and there is a rapid falloff toward the trailing edge. The rate of falloff is attributed to the rapid acceleration of surface flow near the trailing edge toward the trailing-edge sonic point. As the angle of attack increases beyond the shock-detachment angle, free-stream stagnation pressures are present on the $\Lambda = 0°$ plate at approximately 45° angle of attack and with further increase in angle of attack the $\Lambda = 30°$ and 45° plates attain stagnation pressures at angles of attack much less than 90°. At still higher angles of attack the stagnation point moves aft and in a sense both leading and trailing edges are trailing edges as far as the flow is concerned.

The pressure coefficients obtained at each chordwise station (fig. 8) indicate that there is essentially no effect of sweep angle on the two-dimensional pressure distributions on the swept flat plates up to the shock-detachment angle which was calculated, based on a free-stream Mach number of 6.00, to be 31.5° for the 45° swept plate, 37.8° for the 30° swept plate, and 42.4° for the 0° swept plate. Between the angles of 31.5° and 42.4°, the pressure distributions are changing and do not establish a definite trend for all chordwise stations until the angle of attack is increased slightly beyond 42.4°. At this point, the distributions are separated in an orderly manner and show a decrease in local pressure with an increase in sweep angle at a constant angle of attack up to about $\alpha = 70^\circ$ after which sweep effects are negligible.

A better view of the overall effects of sweep angle can be obtained by comparing the maximum measured pressure coefficients. (See fig. 9.) It is clearly shown in the figure that the greatest effects of sweep angle occur near the angle of attack for which shock detachment would be expected on a two-dimensional plate. Thereafter, the maximum pressure coefficients begin to converge. At angles of attack of 70° and above, the pressure coefficients remain constant at the stagnation value of 1.82 for all the flat plates. Stagnation pressures were recorded on the 0° swept model at angles of attack as low as 45°, whereas stagnation pressures were not recorded on the 30° and 45° swept models until angles of attack of about 64° and 70°, respectively.

The modified Newtonian theory using a value of $C_{p,max}$ of 1.818 is presented in figure 9. It is readily seen that the Newtonian prediction is invalid except at $\alpha = 0^\circ$ and 90° and makes no provisions for effects of sweep angle. The flat-plate modified Newtonian theory $\left(C_{p,max} = \gamma + 1\right)$, also shown in figure 9, obtained from reference 6 gives a fair prediction of the measured pressures in the lower angle-of-attack region up to about 40°.

The pressure coefficient, calculated by use of the oblique-shock theory, shows excellent agreement with the measured maximum pressures at lower angles of attack. The theory does, however, slightly underpredict the maximum pressures at angles of attack in a slight region just prior to shock detachment.

Predictions of the maximum pressure coefficient obtained by using an effective Mach number at angles of attack greater than the shock-detachment angle are presented in figure 9 for the three swept plates. This prediction is based on the assumption that, once the body has gone beyond the angle of attack necessary for shock detachment, the component of the free-stream Mach number in the plane normal to the plane containing the plate leading edge will stagnate at some point on the plate as a result of the subsonic flow behind the detached shock. The

stagnation pressure obtained for the 0° swept plate will be a function of the free-stream Mach number; however, the stagnation pressure obtained for the swept plates will be governed by the component of the free-stream Mach number normal to the plate leading edge. By using the equations given in reference 7 for an equivalent two-dimensional flow, an effective Mach number (component of Mach number in the plane normal to the plane containing the plate leading edge) can be computed. If the effective Mach number is known, the total pressure behind a normal shock can be obtained from the fundamental gas-dynamic relations or from a source such as reference 8. With this value of pressure, a pressure coefficient based on free-stream conditions can be computed.

The predictions (fig. 9) are presented as a function of plate angle of attack measured in the plane of the free-stream velocity vector. It can be seen that the predicted values agree fairly well with the measured data. A maximum difference of about 0.1 in C_p is obtained at any point with the exception of regions in the proximity of shock detachment. The trends of the curves of the predicted values and the measured values are approximately the same and indicate that the method and the assumption have some validity.

CONCLUSIONS

The results of an investigation conducted in the Langley 20-inch Mach 6 tunnel on three two-dimensional sharp-leading-edge flat plates with sweep angles of 0°, 30°, and 45° indicate the following conclusions:

1. There is essentially no effect of leading-edge sweep angle on the pressure distributions on the swept flat plates in the attached-shock regime. In the detached-shock regime, the major effects of sweep are generally confined to angles of attack from 43° to 70°.

2. Free-stream stagnation pressures are measured on the 0° swept model at angles of attack as low as 45°, whereas stagnation pressures are not obtained on the 30° and 45° swept models until angles of attack of about 64° and 70°, respectively.

3. Oblique-shock theory gives good predictions of the pressures on the models in the attached-shock regions.

4. Predictions of the maximum plate pressures for the detached-shock regions, obtained by using the Mach number component normal to the plate leading edge, are in fair agreement with measured data.

5. A modified Newtonian theory (maximum pressure coefficient behind a normal shock of 1.818) is ineffective in predicting the maximum measured pressures except at an angle of attack of 90°, whereas the flat-plate modified Newtonian theory gives a fairly good prediction in the low angle-of-attack range up to about 40°.

Langley Research Center,
National Aeronautics and Space Administration,
Langley Station, Hampton, Va., April 27, 1962.

REFERENCES

1. Bertram, Mitchel H., Feller, William V., and Dunavant, James C.: Flow Fields, Pressure Distributions, and Heat Transfer for Delta Wings at Hypersonic Speeds. NASA TM X-316, 1960.

2. Hondros, James G., and Goldberg, Theodore J.: Aerodynamic Characteristics of a Group of Winged Reentry Vehicles at Mach Number 6.01 at Angles of Attack From 60° to 120° and -10° to 30° Roll at 90° Angle of Attack. NASA TM X-511, 1961.

3. Goldberg, Theodore J., and Hondros, James G.: Pressure Distributions on a Flat-Plate Delta Wing Swept 65° at a Mach Number of 5.97 at Angles of Attack From 65° to 115° and Angles of Roll From 0° to 25° at a 90° Angle of Attack. NASA TM X-702, 1962.

4. Sterrett, James R., and Emery, James C.: Extension of Boundary-Layer-Separation Criteria to a Mach Number of 6.5 by Utilizing Flat Plates With Forward-Facing Steps. NASA TN D-618, 1960.

5. Bertram, Mitchel H., and Blackstock, Thomas A.: Some Simple Solutions to the Problem of Predicting Boundary-Layer Self-Induced Pressures. NASA TN D-798, 1961.

6. Grimminger, G., Williams, E. P., and Young, G. B. W.: Lift on Inclined Bodies of Revolution in Hypersonic Flow. Jour. Aero. Sci., vol. 17, no. 11, Nov. 1950, pp. 675-690.

7. Shapiro, Ascher H.: The Dynamics and Thermodynamics of Compressible Fluid Flow. Vol. II. The Ronald Press Co., c.1954, p. 710.

8. Ames Research Staff: Equations, Tables, and Charts for Compressible Flow. NACA Rep. 1135, 1953. (Supersedes NACA TN 1428.)

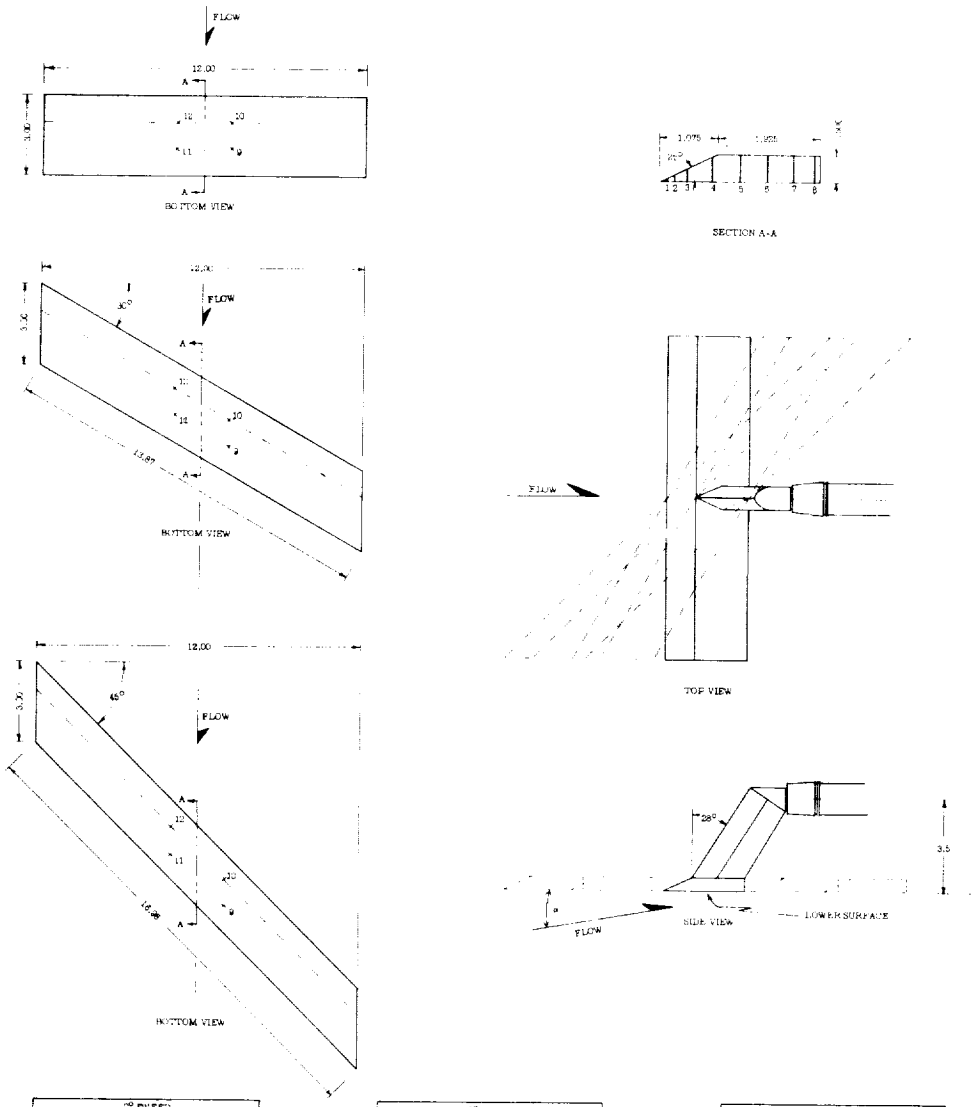

0° SWEEP		
ORIFICE	DISTANCE FROM —	
	LEADING EDGE	CENTER LINE
1	0.138	0.000
2	.251	0.000
3	.517	0.000
4	1.001	0.000
5	1.497	0.000
6	2.001	0.000
7	2.498	0.000
8	2.893	0.000
9	1.000	1.000
10	1.000	1.000
11	1.007	1.000
12	1.000	1.000

30° SWEEP		
ORIFICE	DISTANCE FROM —	
	LEADING EDGE	CENTER LINE
1	0.144	0.000
2	.289	0.000
3	.539	0.000
4	1.001	0.000
5	1.505	0.000
6	2.004	0.000
7	2.498	0.000
8	2.904	0.000
9	2.008	1.000
10	1.007	1.000
11	1.987	1.000
12	1.009	1.000

45° SWEEP		
ORIFICE	DISTANCE FROM —	
	LEADING EDGE	CENTER LINE
1	0.137	0.000
2	.263	0.000
3	.519	0.000
4	.998	0.000
5	1.498	0.000
6	2.006	0.000
7	2.500	0.000
8	2.922	0.000
9	2.015	1.000
10	1.015	1.000
11	2.007	1.000
12	.994	1.000

Figure 1.- Dimensions and orifice locations of two-dimensional swept-flat-plate models. All dimensions are in inches unless otherwise indicated.

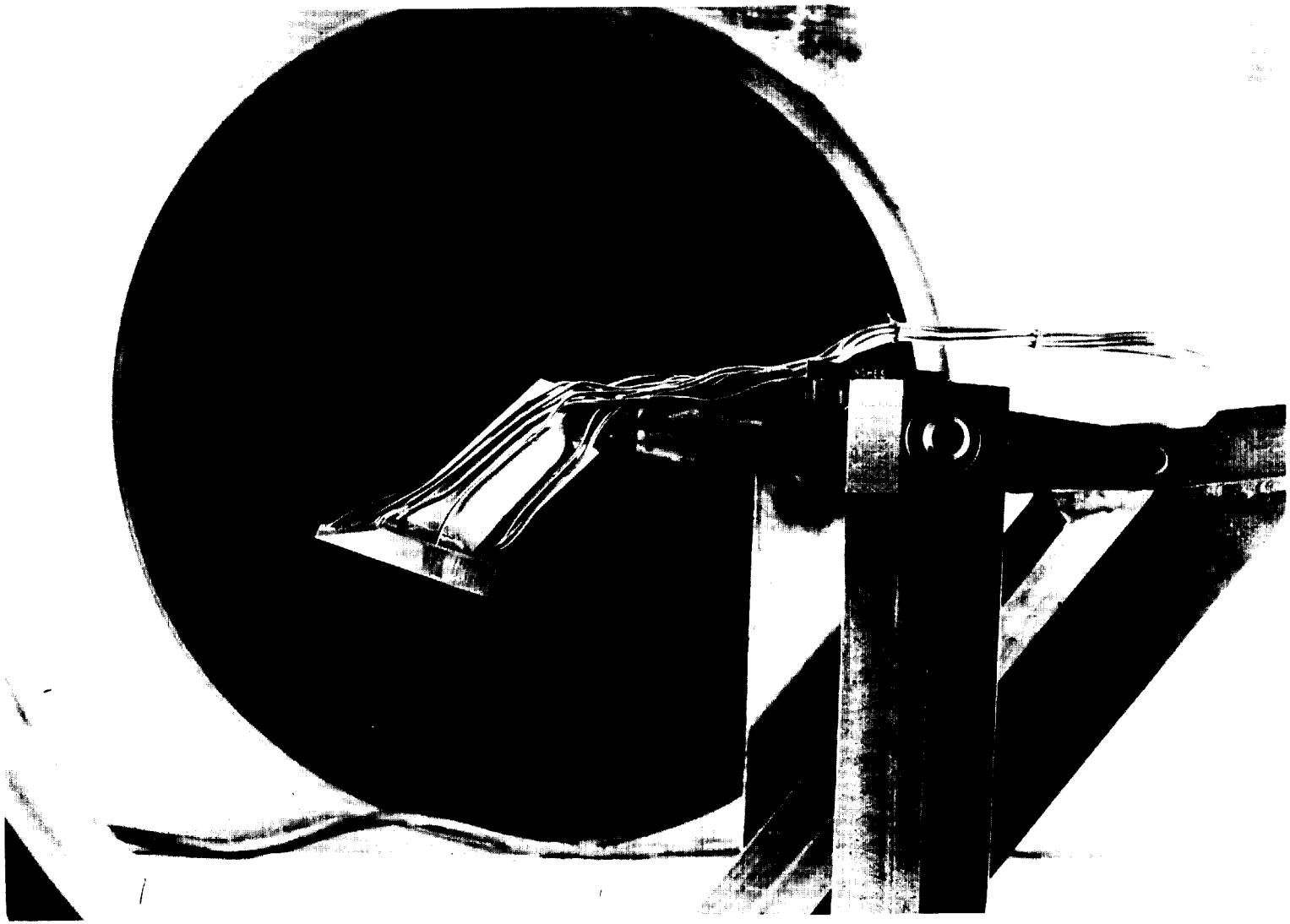

L-62-383

Figure 2.- The 0° swept model mounted on the 90° angle-of-attack support system.

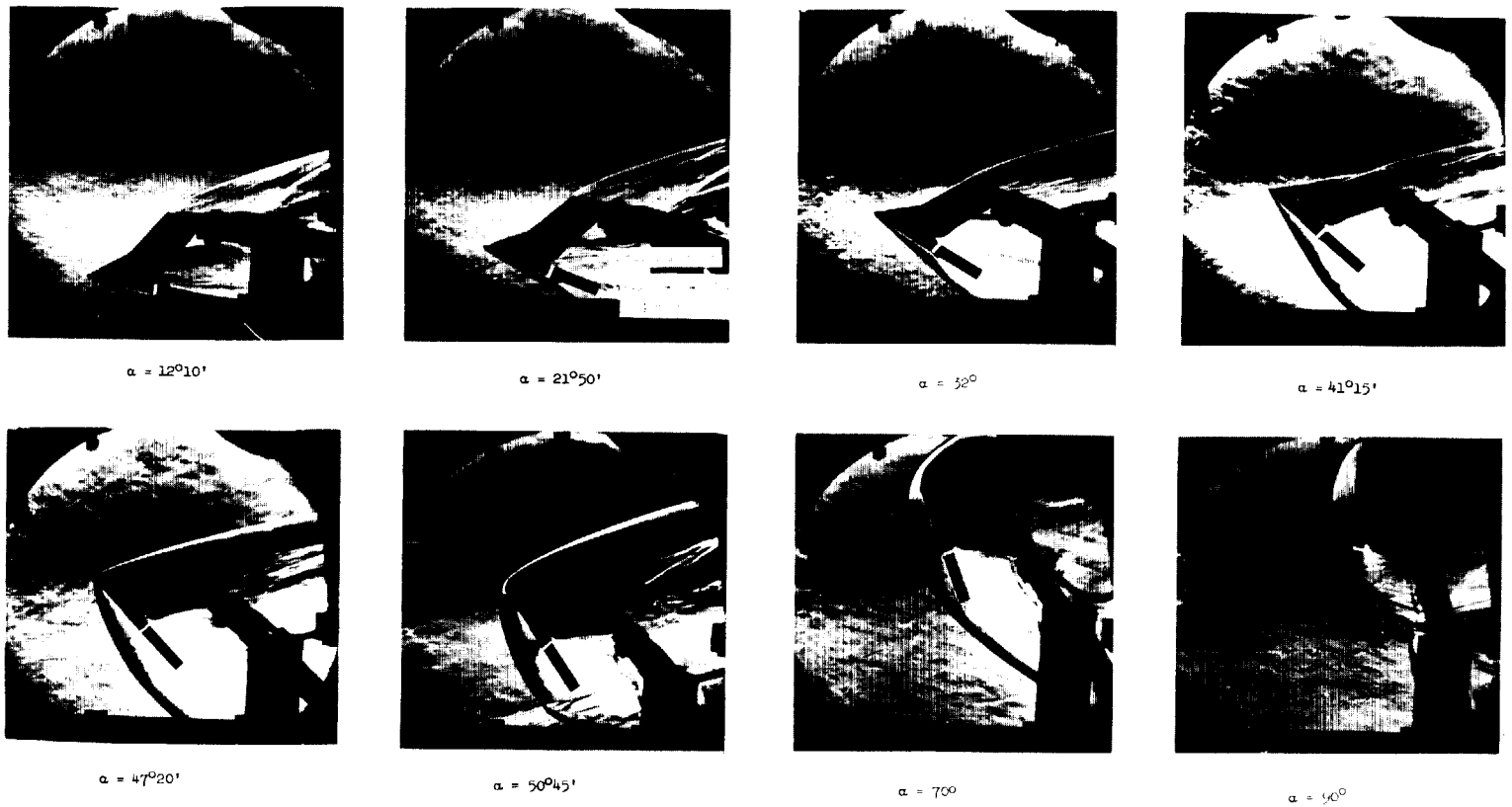

Figure 3.- Typical schlieren photographs of 0° swept model. L-62-2055

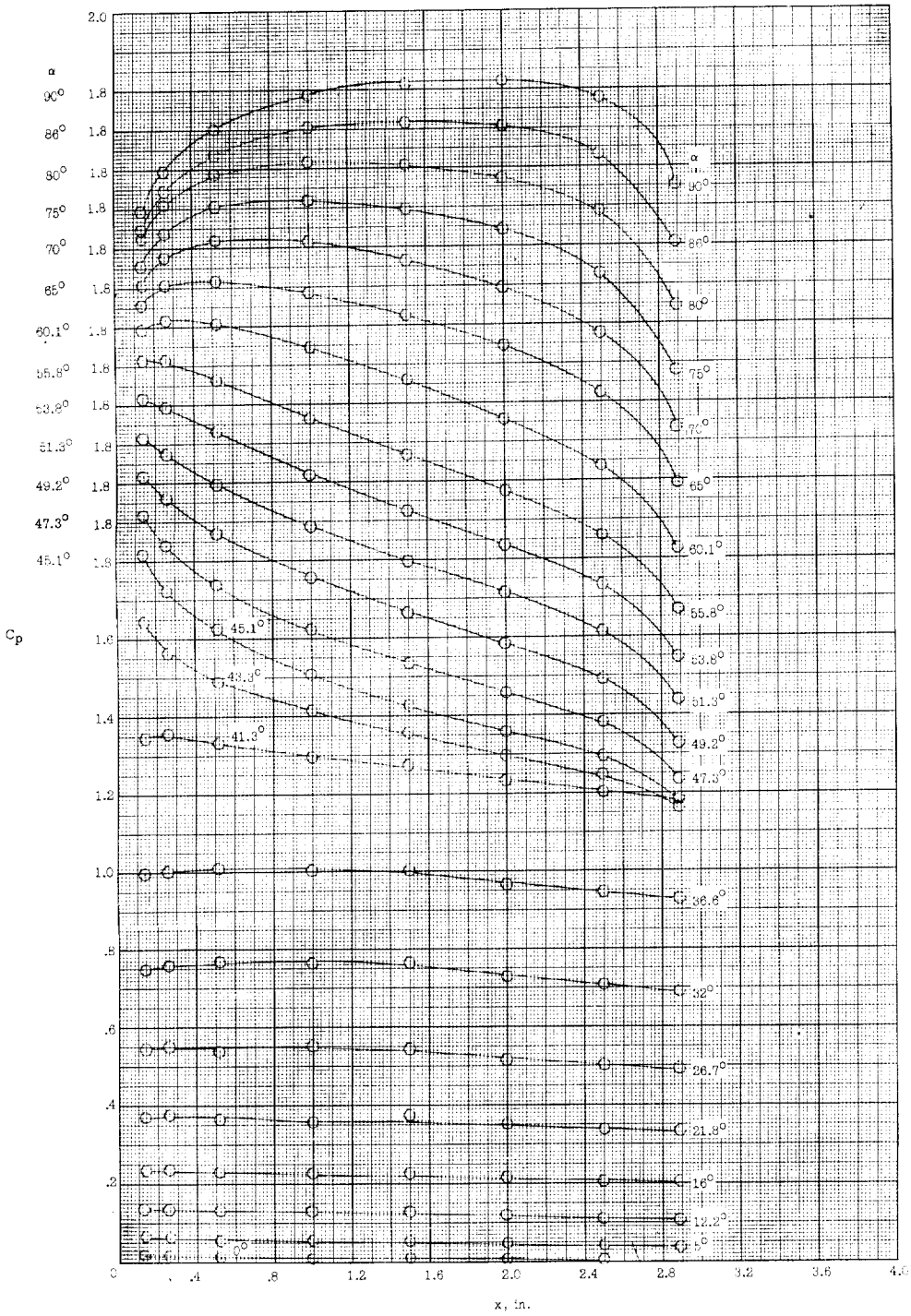

Figure 4.- Pressure distributions on the 0° swept model at angles of attack.

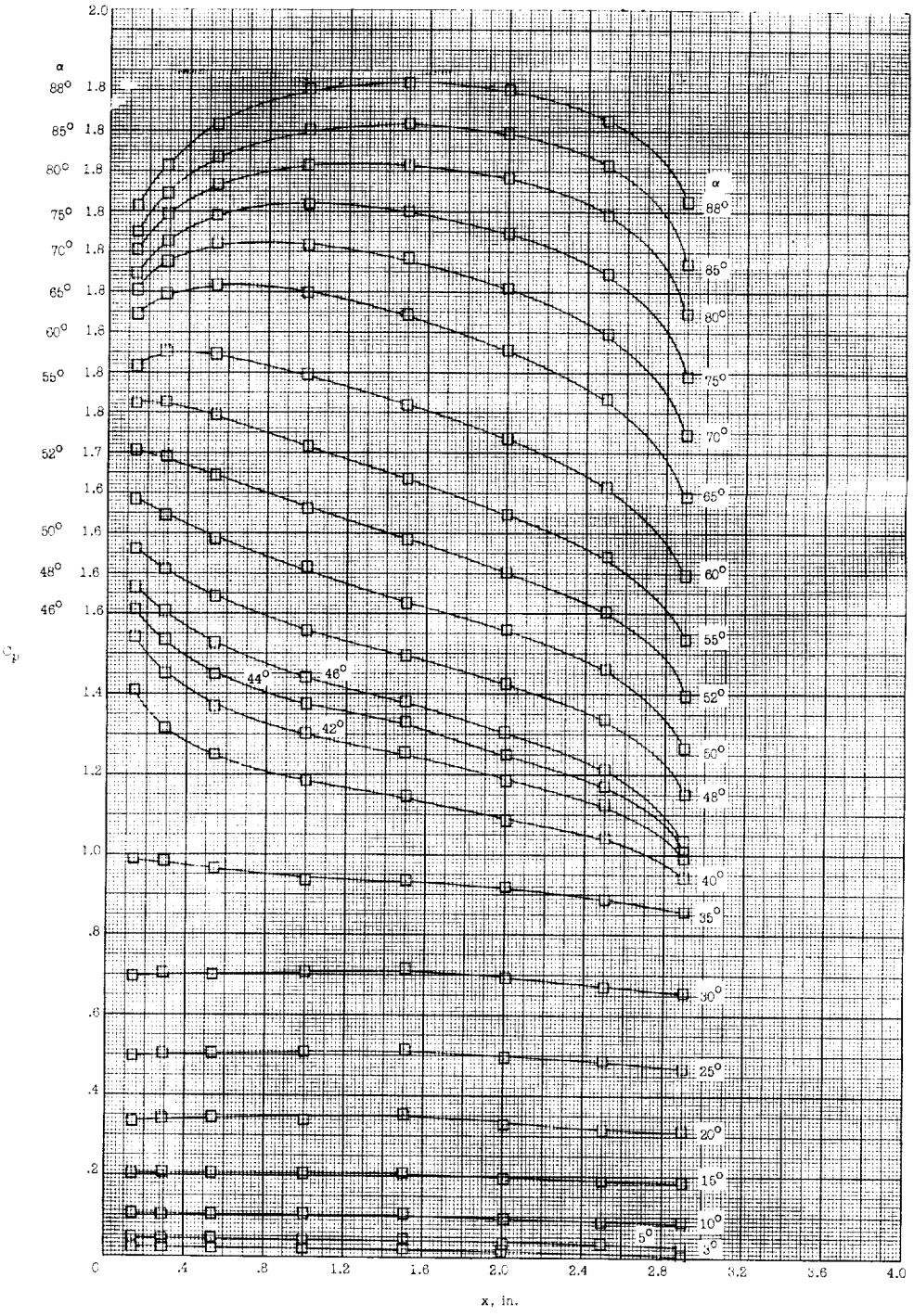

Figure 5.- Pressure distributions on the 30° swept model at angles of attack.

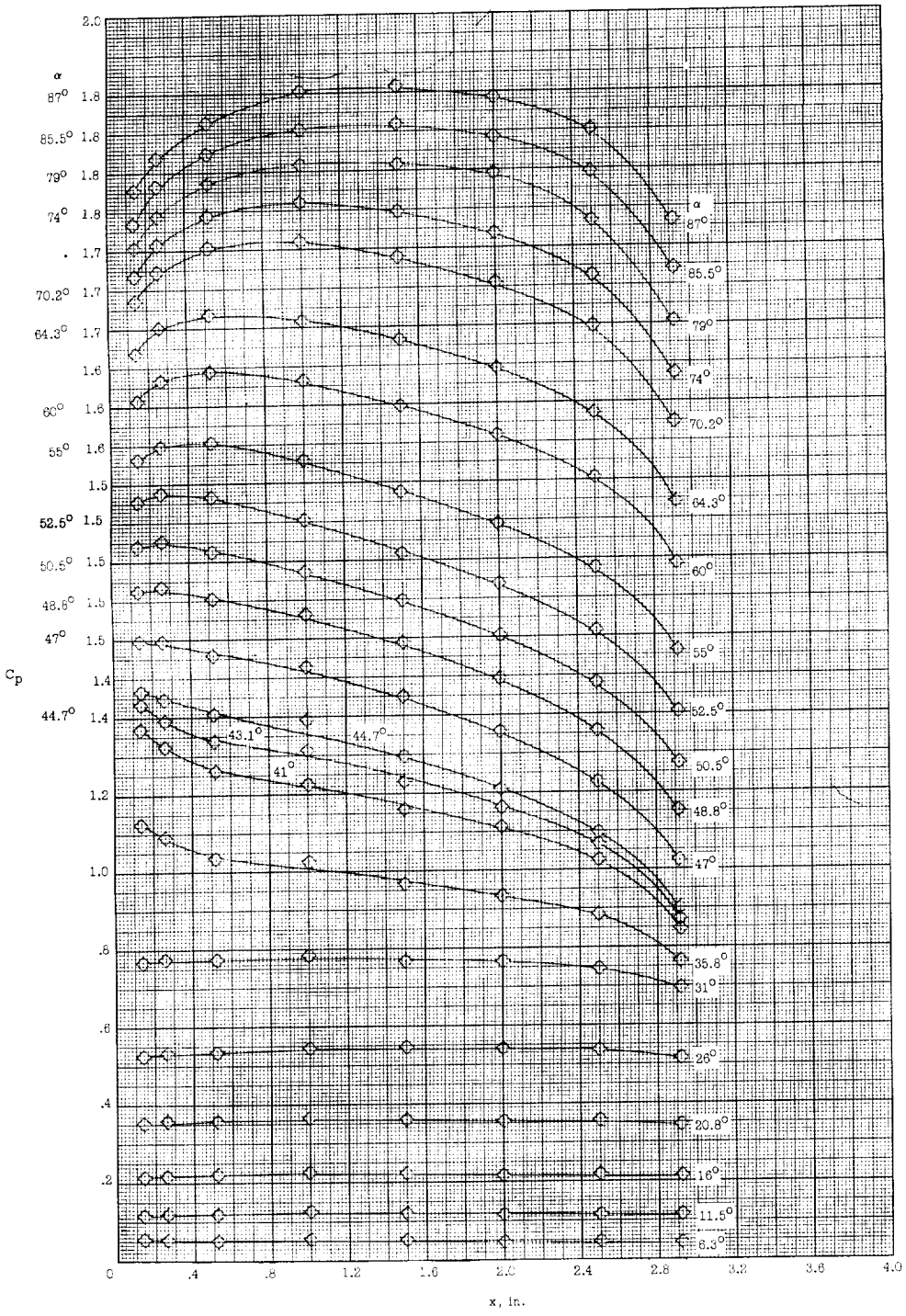

Figure 6.- Pressure distributions on the 45° swept model at angles of attack.

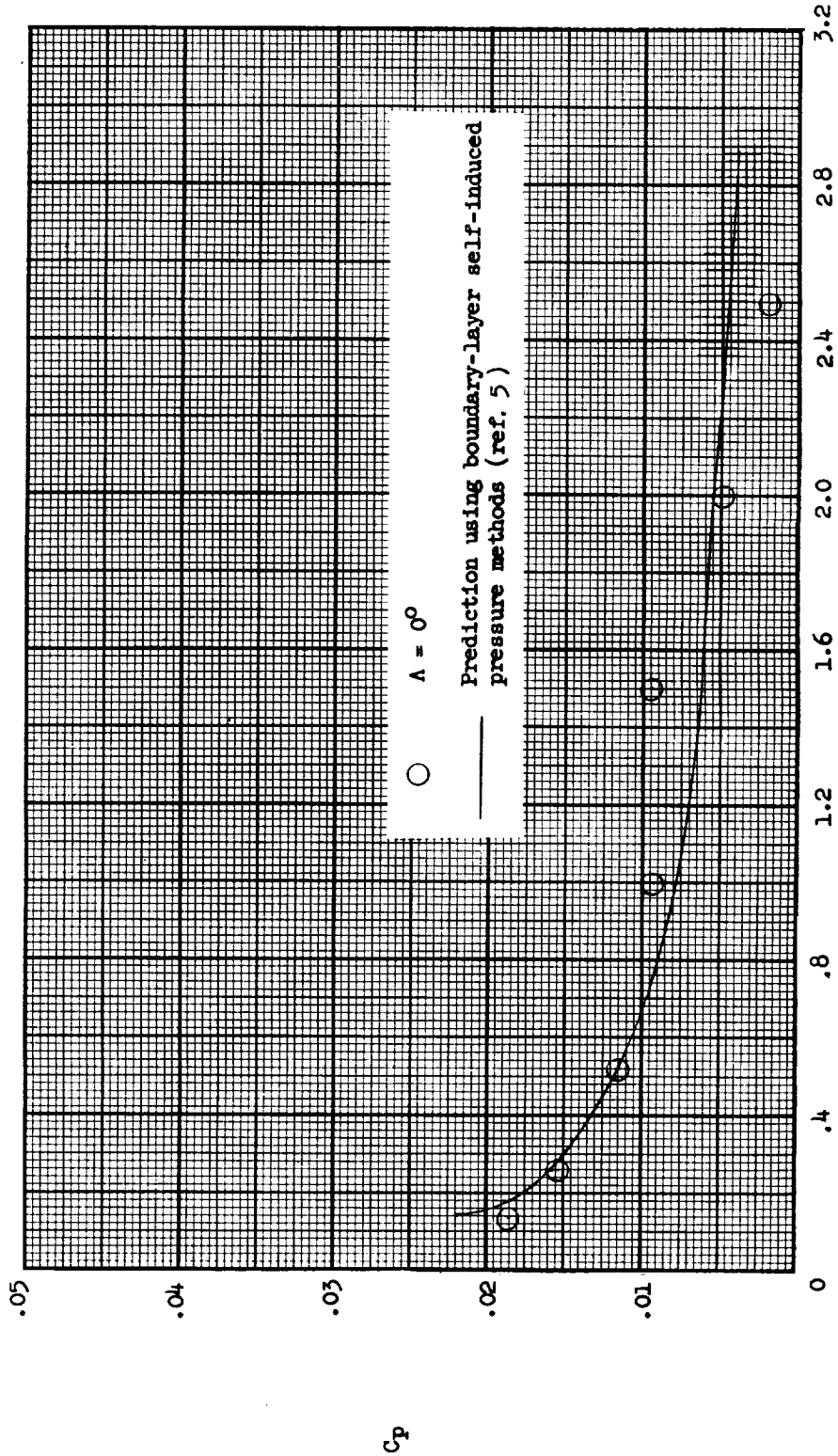

Figure 7.- Pressure distributions at 0° angle of attack.

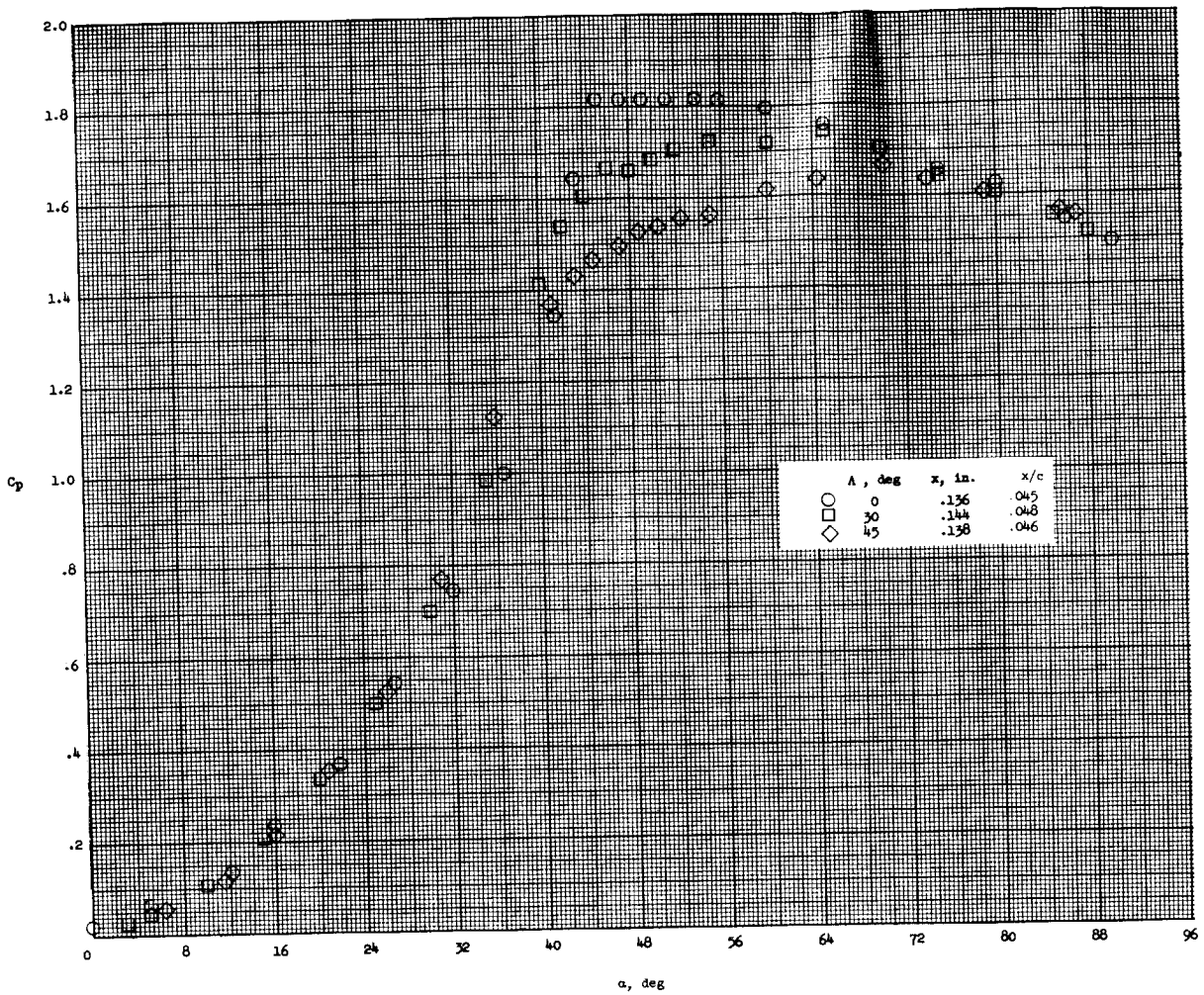

(a) $x/c \approx 0.05$.

Figure 8.- Pressure distributions at an approximately constant chord station at angles of attack.

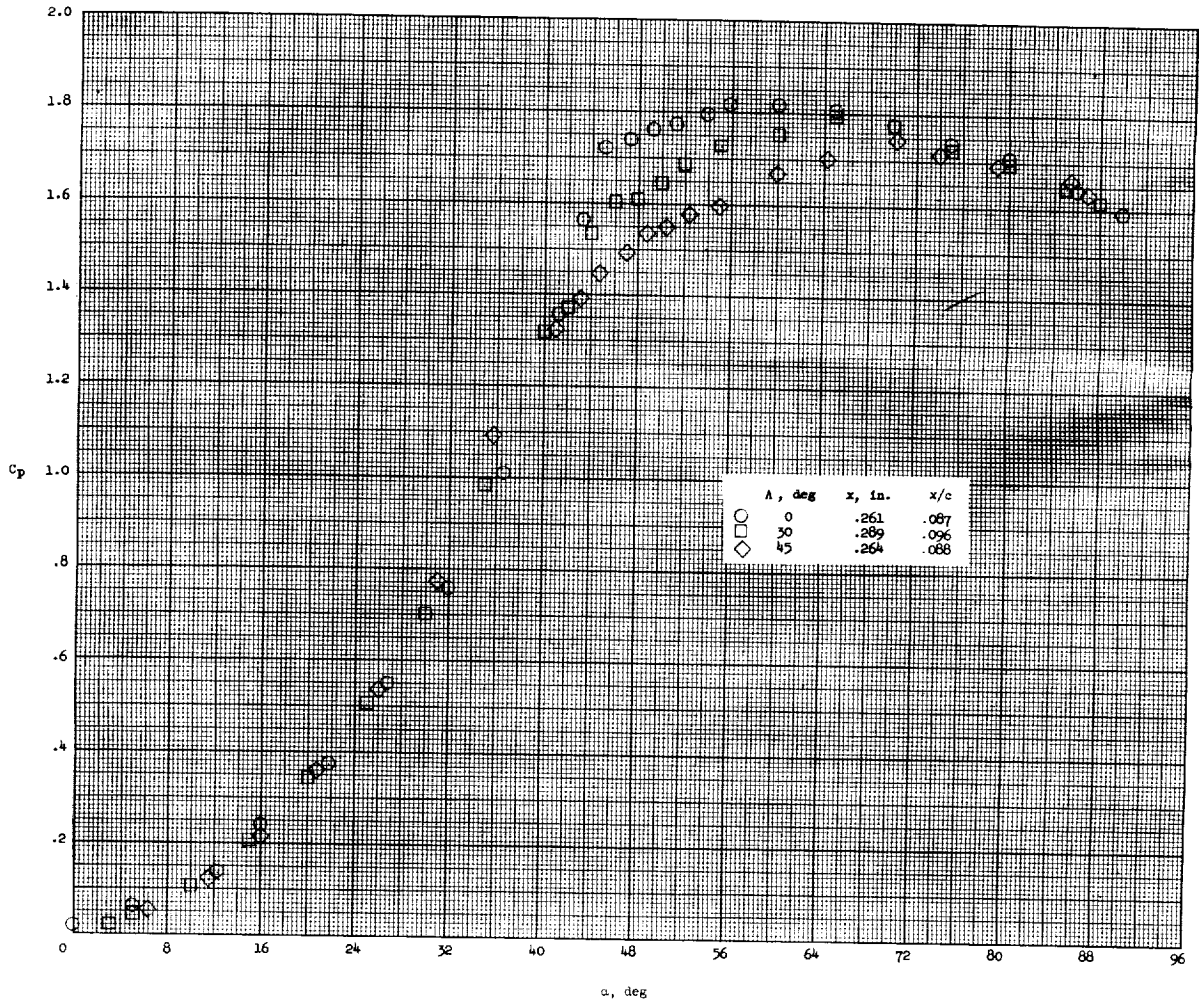

(b) $x/c \approx 0.09$.

Figure 8.- Continued.

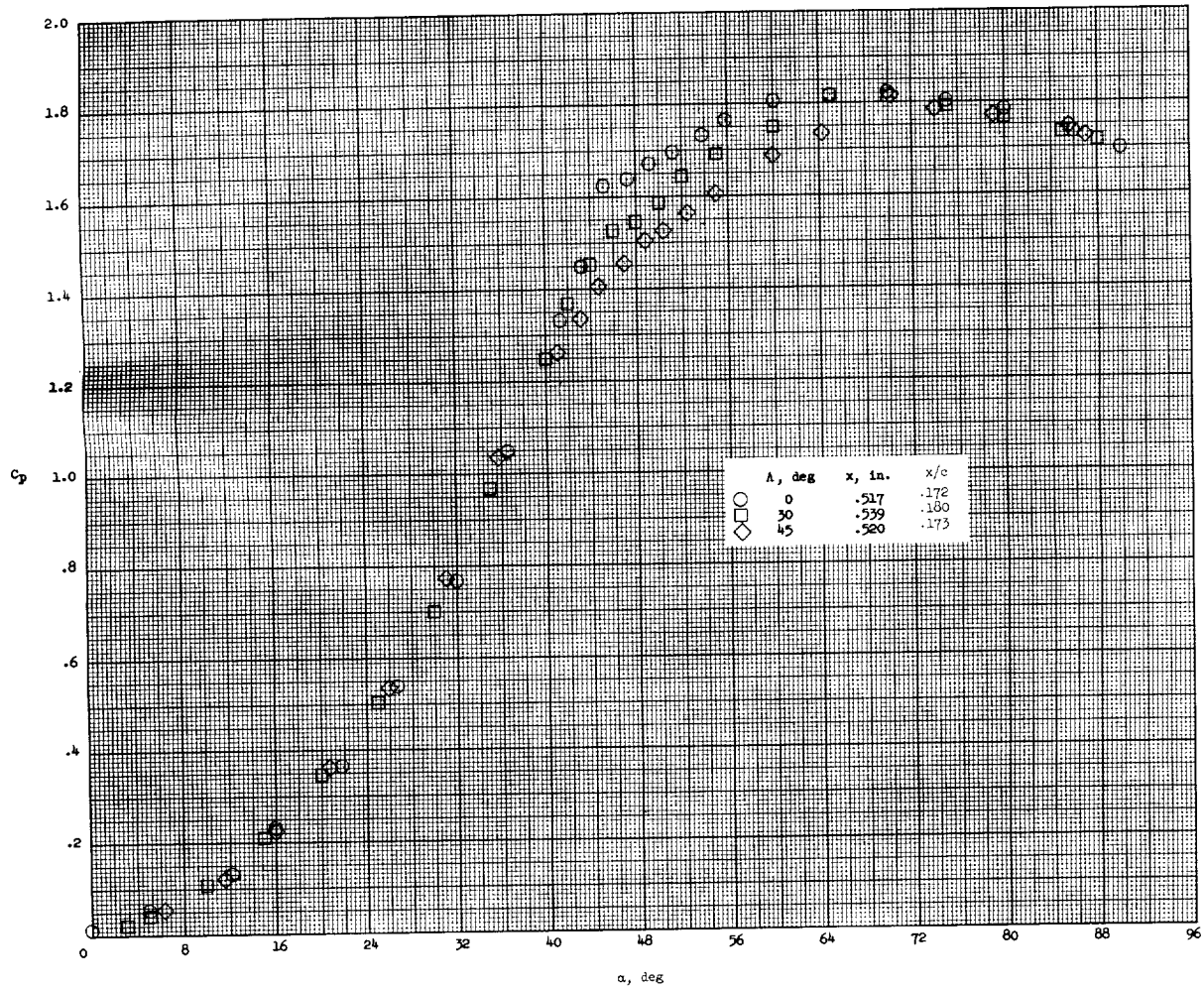

(c) $x/c \approx 0.17$.

Figure 8.- Continued.

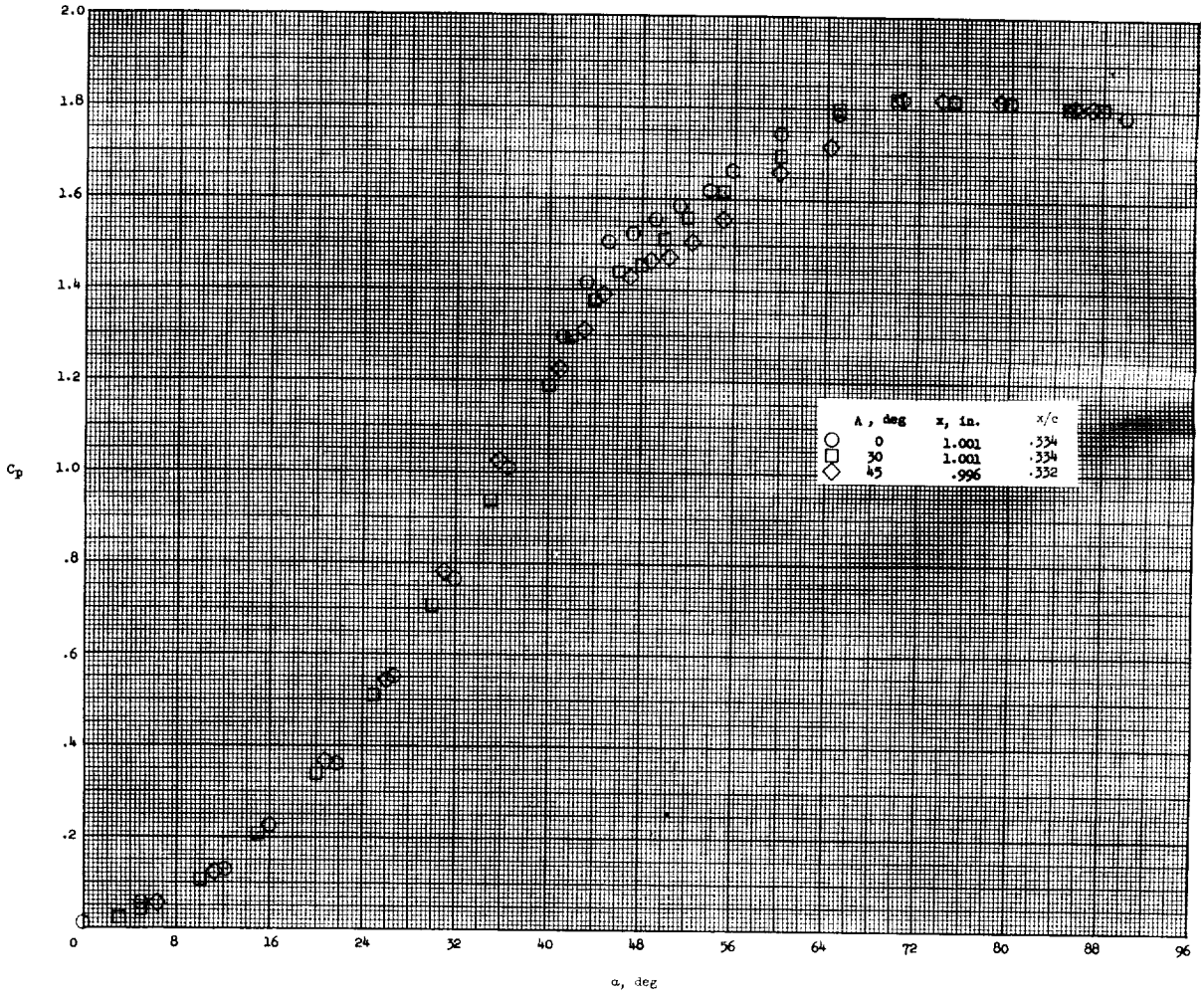

(d) $x/c \approx 0.33$.

Figure 8.- Continued.

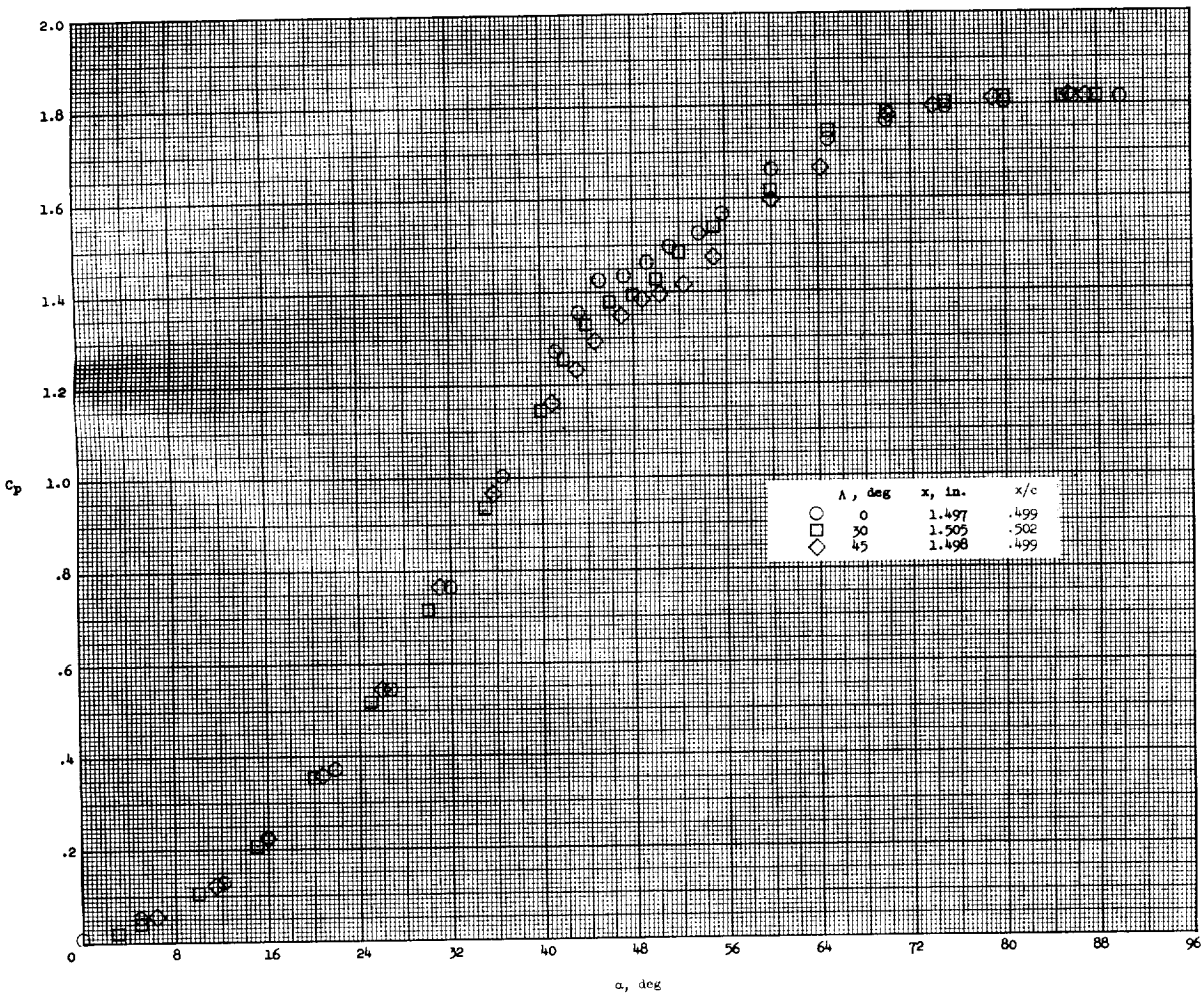

(e) $x/c \approx 0.50$.

Figure 8.- Continued.

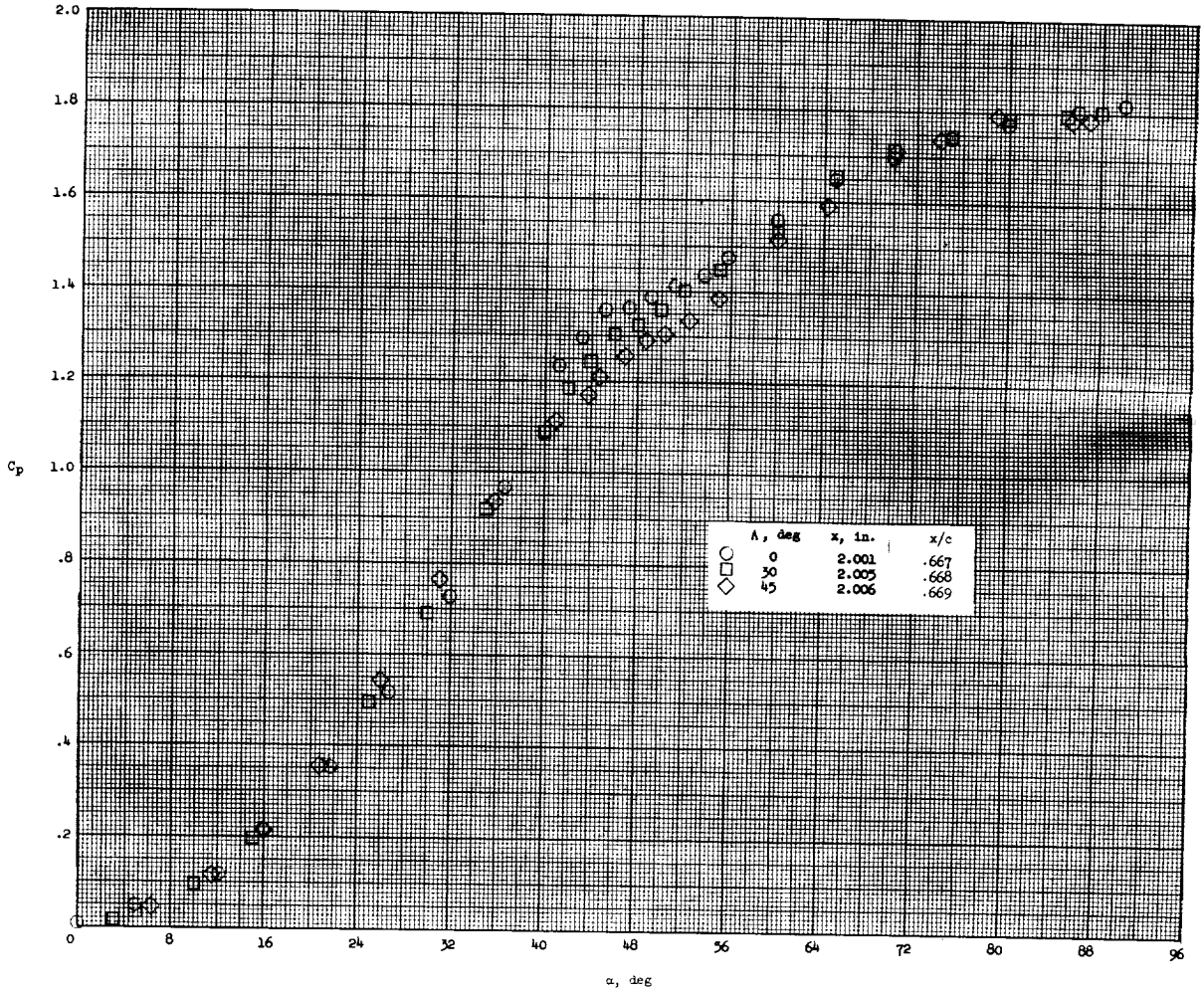

(f) $x/c \approx 0.67$.

Figure 8.- Continued.

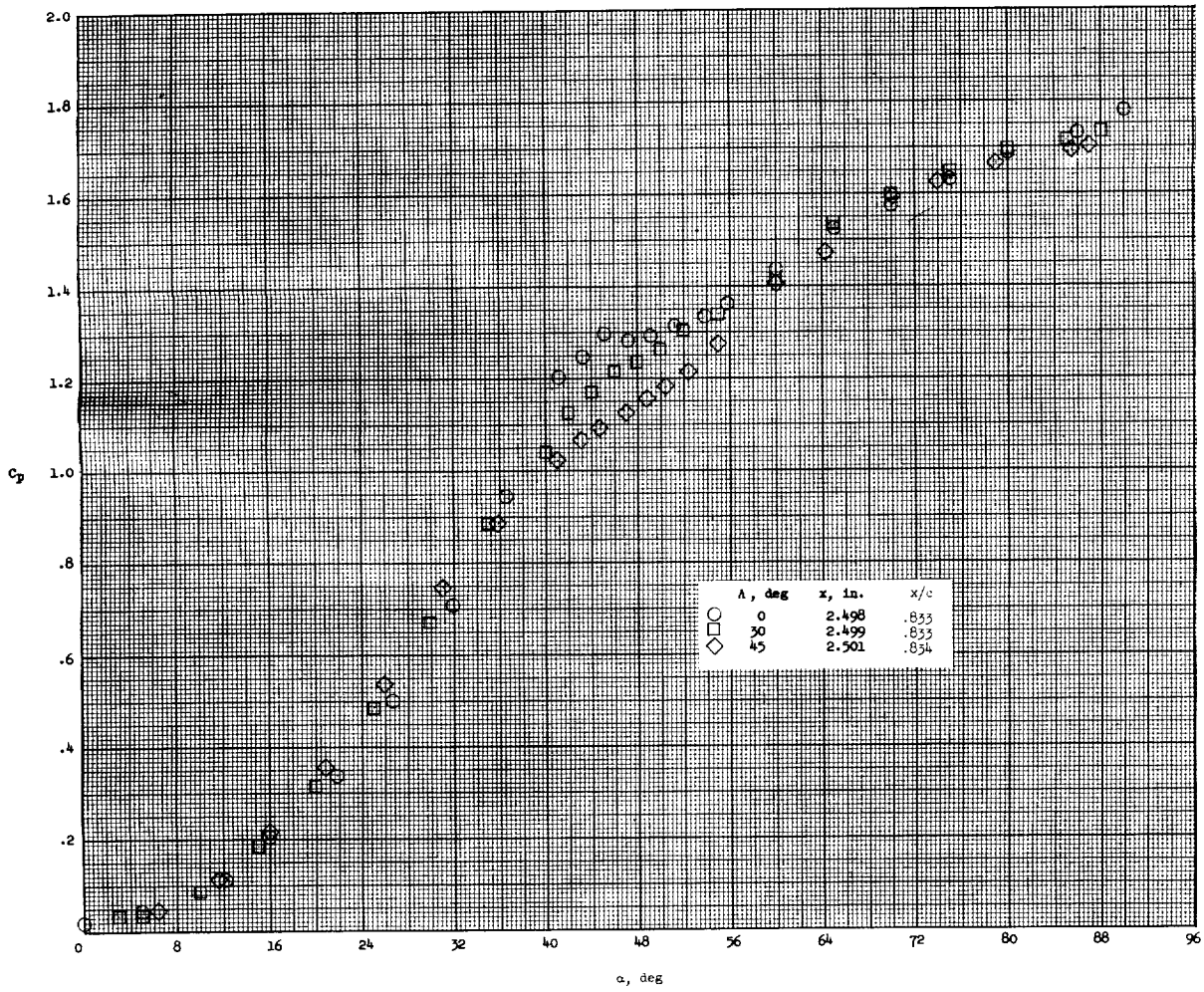

(g) $x/c \approx 0.83$.

Figure 8.- Continued.

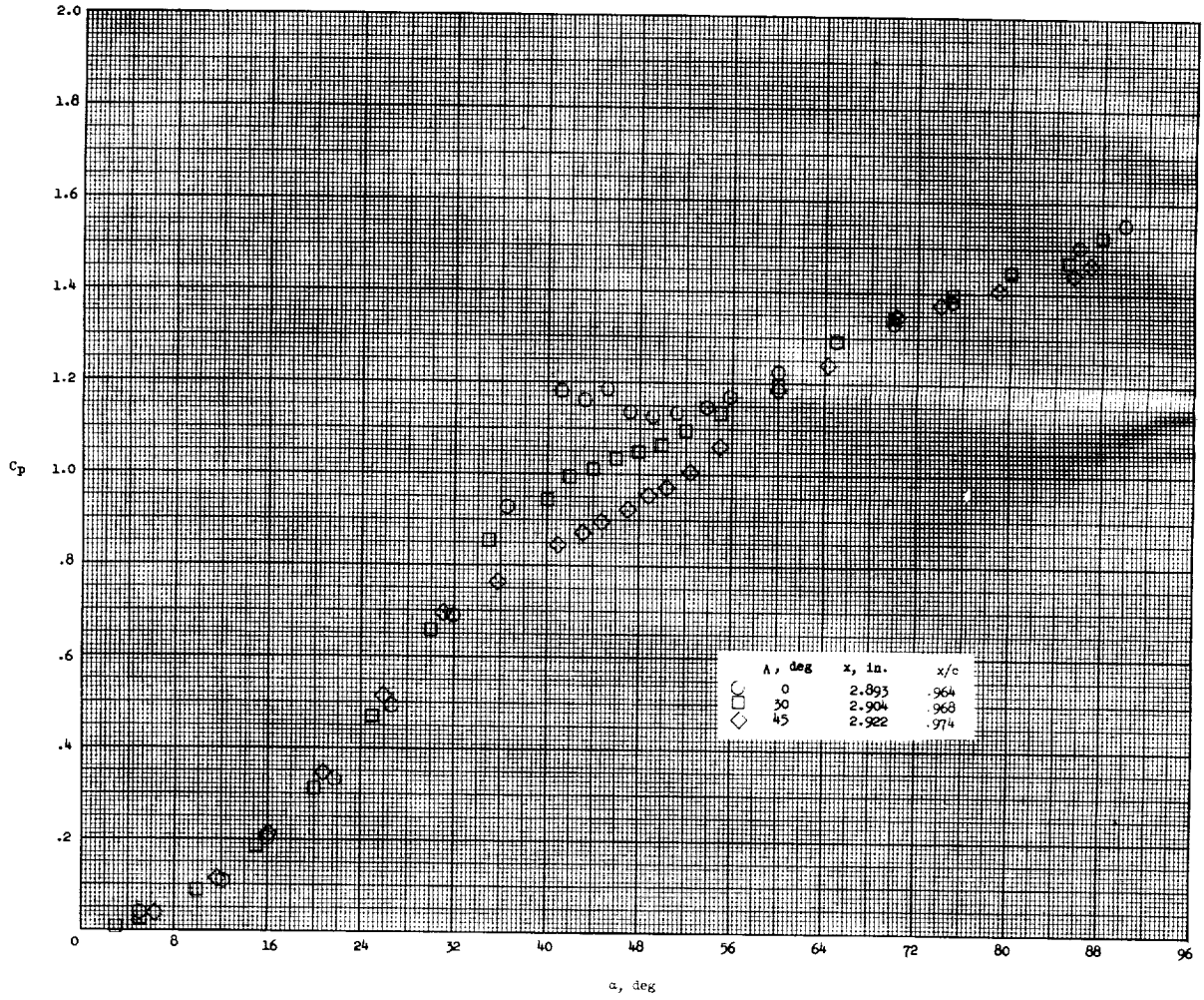

(h) $x/c \approx 0.97$.

Figure 8.- Concluded.

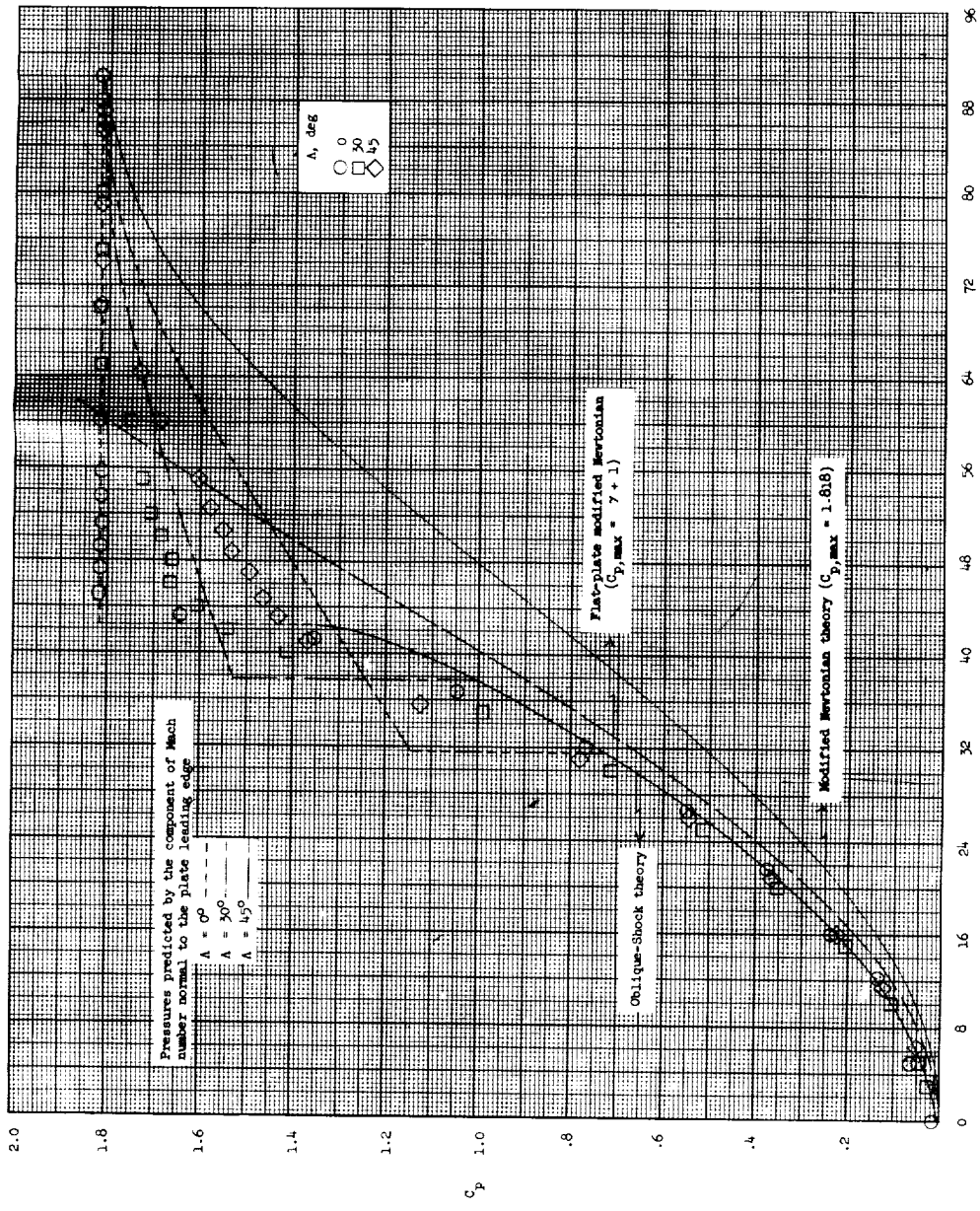

Figure 9.- Predictions and comparisons of maximum measured pressures on the 0°, 30°, and 45° swept models at angles of attack.

NASA-Langley, 1962 L-2077